

## A Low Friction Demanding Approach in Gait Planning for Humanoid Robots During 3D Manoeuvres

Majid Khadiv, S. Ali A. Moosavian\*

*Center of Excellence in Robotics and Control, Advanced Robotics & Automated Systems (ARAS) Laboratory,  
Department of Mechanical Engineering, K. N. Toosi University of Technology, Tehran, Iran.*

Received 6 September 2014; Accepted 6 October 2014

### Abstract

This paper proposes a gait planning approach to reduce the required friction for a biped robot walking on various surfaces. To this end, a humanoid robot with 18 DOF is considered to develop a dynamics model for studying various 3D manoeuvres. Then, feasible trajectories are developed to alleviate the fluctuations on the upper body to resemble human-like walking. In order to generate feasible walking patterns, not only horizontal interaction moments for the computation of ZMP, but also horizontal forces and vertical moment constraints between the feet and the ground surface are taken into account. Since the pelvis trajectory does drastically affect the walking pattern, the focus will be on generating a smooth motion for the pelvis. This smooth motion is generated based on a desired motion for the robot's Centre of Mass (COM), which is mapped to the joint space using inverse kinematics. In fact, the proposed approach involves computing a moving ZMP based on a predefined desired COM trajectory to reduce the required friction for stable walking. The suggested gait planning approach (Low Friction Demanding Moving-ZMP, LFDm) is compared to various existing approaches considering slippage conditions. The obtained results reveal the effectiveness of the proposed method for various walking speeds which will be discussed.

**Keywords:** *biped robots; feasible motion; gait planning; slippage effects.*

### 1. Introduction

Thanks to substantial improvements in technology during the past two decades, the world of humanoid robotics has experienced significant advances. This is perhaps due to improvements in actuators, sensors and processors. However, many unsolved problems

in this field have persuaded many researchers around the world to focus more on this subject.

Because of the unilateral contact between the feet and the ground surface, one of the most significant challenges in this field is generating feasible walking patterns. Many parameters are involved in the procedure of gait planning, so may be exploited to optimize some cost functions. Many research studies have been performed focusing on minimizing the energy

---

\* Corresponding Author. Tel: +98 21 8406 3238  
E-mail: moosavian@kntu.ac.ir

consumption of the humanoid robots' motion within the frame of optimal control theory. Rostami et al. exploited the Pontryagin Maximum Principle (PMP) to globally minimize the joint space torques rather than energy expenditure [1]. Furthermore, Capi et al. used the same approach to generate energy optimistic motion with minimized torque fluctuations [2]. Bessonnet et al. stated the problem of dynamic-based optimization through spline based parametric optimization [3]. In all of these research studies the problem of gait planning involves searching through feasible motions that satisfy dynamic balance constraints using the robot's dynamics model. However, using such a model to generate feasible motion is computationally a demanding approach, and less intuitive.

To generate feasible walking patterns, most researchers use reference points rather than a dynamics model, to satisfy dynamic balance constraints. The most famous reference point is certainly the Zero Moment Point (ZMP) introduced by Vokubratovic [4]. The ZMP represents a point on the ground surface where the horizontal components of the resultant moments of all external forces become zero. If this point remains inside the support polygon during walking, this motion would be dynamically balanced. Furthermore, Goswami introduced another reference point, called the Foot Rotation Indicator (FRI) [5]. The FRI is a point on the ground where the reaction force should be exerted so that the robot remains dynamically balanced. Unlike the ZMP, the FRI can be outside of the borders of the support polygon [6].

In the case of using ZMP to generate feasible motion, two approaches are usually adopted. The first approach uses the complete information of the model such as masses and moments of inertia, and the locations of the COM of the links to calculate the ZMP using a multi-body model. In this notion, Huang et al. related the problem of gait planning to search through the hip trajectories that generate patterns with a maximum stability margin [7]. Dau et al. used this approach to generate an energetically efficient feasible motion by considering seven key parameters and optimization using a Genetic Algorithm (GA) [8]. Although by using a multi-mass model, the

accurate position of the ZMP can be computed, the calculation burden is considerable and this method cannot be used in real time gait planning.

In order to generate a real time trajectory for a biped, a simple model is introduced by Kajita et al., called the Linear Inverted Pendulum Model (LIPM) [9]. In this model the whole body of the robot is considered as a concentrated mass connected to the ground surface at the ZMP, using a massless link. In this approach, the linear differential equation is solved to calculate the COM trajectory from a predefined ZMP trajectory. Erabtor et al. used a Fourier transform and a Lanczos sigma to estimate the smooth and continuous trajectory for the ZMP and generate the COM trajectory by solving the LIPM equations [10]. Moosavian et al. used a shooting method to solve the Initial Value Problem (IVP) of the LIPM and to generate feasible patterns for walking on uneven terrains [11]. However, in LIPM the height of the COM is limited so as to be fixed during walking. Hence, Huang et al. adopted the original nonlinear inverted pendulum model to generate a walking pattern with a changeable height of the COM [12]. Because the approximation of the multi-body humanoid robot with an inverted pendulum is used in this method, the error between the desired and actual ZMP can be large, in reality. To cope with this problem, Suleiman et al. used system identification techniques to increase the accuracy of the inverted pendulum model. [13] Furthermore, the two masses model [14], and the three masses model [15] have been adopted as the generalization of the single mass model to describe the motion more precisely. The walking patterns that are generated in the task space are projected into the joint space using inverse kinematics [16]. Then, the controller in the lowest level of the hierarchy of the control structure guarantees that the trajectories in the joint space [17, 18] or the task space [19] would be tracked.

In all of the aforementioned research studies, it is assumed that there exists enough friction between the feet and the ground surface to implement the motion. For the gait planning procedure, few research studies discuss the desired horizontal forces and the vertical moment that are exerted by the ground surface

to the feet. Aside from some research studies which focus on exploiting the slip to generate some motions like turning [20], others study slippage effects as harmful phenomena. Boone et al. examined the walking of biped robots on slippery surfaces, and proposed some strategies in their online controller structure to recover the robot when a slip occurs [21]. This controller was based on model-independent reflexive actions. Park and Kwon simulated the motion of a 12 degrees of freedom (DOF) biped robot on slippery surfaces [22]. They designed a controller that increases the friction force at the occasion of the slip. Kajita et al. presented a method that can be implemented in terrain with a low friction coefficient [23]. They used a cart-table model as a simple model to cope with horizontal forces acting on the stance feet. Kaneko et al. considered a slip observer and stabilizer in their online controller topology [24]. In their structure, the slip observer detects the slip and the stabilizer compensates the errors that occur due to the slip. Zhou et al. distinguished the translational and rotational motion of the feet due to the slip [25]. They suggested that in some situations the rotational motion is more important than the translational motion of the feet during the slip.

Based on the above, a thorough analysis on the slippage effects of the stance foot should be performed during gait planning, which is the focus of this paper. In fact, most research studies which have been done in the area of feasible gait planning for biped robots assume enough friction exists between the feet and the

ground surface. However, humanoid robots should perform in an outdoor environment which may be slippery. Hence, in this paper a novel gait planning approach is proposed which demands low friction forces, and so it is suitable for walking on slippery surfaces. Therefore, the main contribution of this paper is to examine the effects of the slip on humanoid walking patterns, and to present a method to reduce the demanding friction force for stable walking. The rest of this paper is as follows: in section (2) a verified dynamics model for the considered robot is developed. Section (3) is allocated to the slip considerations and friction modelling to be exploited in the gait planning procedure. Section (4) describes generating trajectories in a Cartesian space to implement feasible motion. In section (5), the obtained results are discussed.

## 2. Dynamics Model

In this paper an 18 DOF humanoid robot is studied, Figure 1. The kinematic structure of the robot, and its links and joints are specified in Figure 1, where each leg has six DOF and each arm has three DOF. In this section, the equations of the motion of the robot during both the single and double support phases are developed. In order to state the equations in a form that is valid for all the phases, the robot is considered as a free body without any contact with the environment. Then, using compatible constraints in each phase, the constrained dynamics model can be obtained.

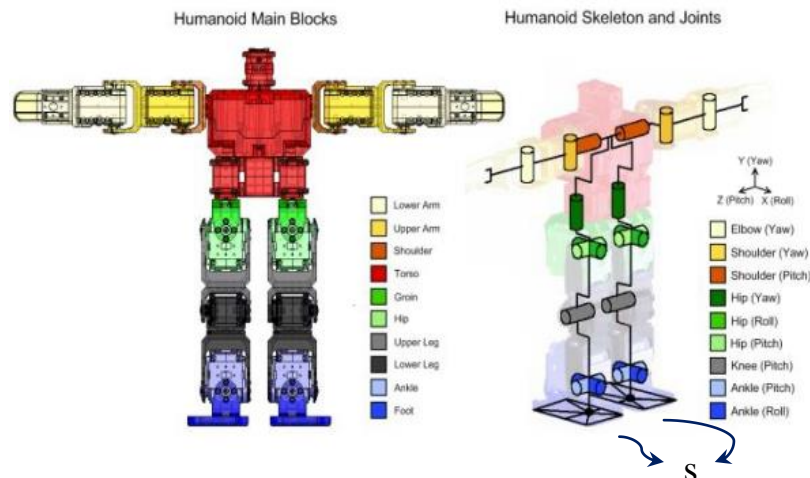


Fig. 1. Under-study humanoid robot with 18 DoF

Considering the pelvis posture  $[q_p]_{6 \times 1}$ , the relative right and left leg joints' angles  $[q_{R-L}]_{6 \times 1}$  and  $[q_{L-L}]_{6 \times 1}$  and the relative right and left arm joints' angles  $[q_{R-A}]_{3 \times 1}$  and  $[q_{L-A}]_{3 \times 1}$ , the generalized coordinates vector can be written as:

$$q_{24 \times 1} = [q_{R-A} \ q_{R-L} \ q_P \ q_{L-A} \ q_{L-L}]^T \quad (1)$$

The equations of the motion for the robot which interacts with its environment may be written as the set of equations:

$$M_{24 \times 24}(q) \ddot{q}_{24 \times 1} + C_{24 \times 1}(q, \dot{q}) + G_{24 \times 1}(q) = Q_{24 \times 1} \quad (2)$$

In this set of equations, the first term on the left hand side represents inertia effects, the second term is composed of the Coriolis and centrifugal effects, and the third term represents gravity effects. The right hand side can be formulated as:

$$Q_{24 \times 1} = B_{24 \times 18} \tau_{a_{18 \times 1}} + J_{v_{24 \times 3}}^\tau F_{E_{3 \times 1}} + J_{\omega_{24 \times 3}}^\tau M_{E_{3 \times 1}} \quad (3)$$

where  $\tau$  is a vector, which includes the joints, actuating torques. Furthermore,  $B$  is a constant matrix which projects joints' actuating torques to the space of the generalized coordinates.  $F_E$  and  $M_E$  represent the force and moment vectors which are applied by the ground surface, in interaction points, and  $J_v$  and  $J_w$  represent the linear and angular Jacobian matrices of the contact points, respectively. The first term of this equation is actuating joint torques, the second and third terms are interaction forces and moments respectively, which are mapped into the joint space using Jacobian matrices

### 2.1. Single support phase

In the single support phase (SSP), it is assumed that the stance foot is fixed on the ground. As long as the forces and moments acting on the feet do not exceed a tolerable bound, this assumption is valid. The bound for these forces can be obtained using dynamic balance equations that will be specified in the next sections. Moreover, in order to guarantee that the stance foot does not slip, the friction forces

between the feet and the ground should be enough. These conditions will be discussed in sections 3 and 4, completely. Under such circumstances, these assumptions can be represented as holonomic constraints:

$$\begin{bmatrix} X_s - C \\ \theta_s \end{bmatrix}_{6 \times 1} = 0 \quad (4)$$

In this set of equations  $C$  is constant and  $X_s$  and  $\theta_s$  represent the position and orientation of the point on the stance foot just below the ankle joints intersection which is specified in Figure 1.

Using the constraint relaxation method, [26] equal with constraints represented in Equation 5, the forces and moments exerted on the point  $s$  from the ground surface can be written as:

$$f_s = \begin{bmatrix} F_s \\ M_s \end{bmatrix}_{6 \times 1} \quad (5)$$

The Jacobian matrix of this point of the stance foot can be written as:

$$J_s = \begin{bmatrix} J_v \\ J_w \end{bmatrix}_{6 \times 24} \quad (6)$$

Substituting Equations 5 and 6 into 3 and 2, the dynamics model in SSP can be specified:

$$M_{24 \times 24}(q) \ddot{q}_{24 \times 1} + C_{24 \times 1}(q, \dot{q}) + G_{24 \times 1}(q) = B_{24 \times 18} \tau_{a_{18 \times 1}} + J_{s_{24 \times 6}}^T f_{s_{6 \times 1}} \quad (7)$$

In order to solve these equations for the actuating torques and interaction forces and moments, by manipulating the above set of equations we have:

$$\begin{bmatrix} \tau_a \\ f_s \end{bmatrix}_{24 \times 1} = \begin{bmatrix} B & J_s^T \end{bmatrix}_{24 \times 24}^{-1} \left( M_{24 \times 24}(q) \ddot{q}_{24 \times 1} + C_{24 \times 1}(q, \dot{q}) + G_{24 \times 1}(q) \right) \quad (8)$$

By substituting the joint space trajectories, the right hand side of the set of the above equations is known and the set of algebraic equations can be solved for actuating torques and interaction forces and moments.

### 2.2. Double support phase

In our gait planning procedure, during DSP, one of the feet is completely in contact with the ground while the other foot rotates around

either the heel or the toe edge. Thus, the constraints on each foot are different. For the foot that is completely in contact with the ground surface, the constraints are exactly the same as the constraints on the stance foot during SSP. For the other foot, the constraints can be stated for the edge in contact with the ground. For this edge, all of the posture elements are zero except for the rotation around the toe or heel edge which is in contact with the environment. This set of constraints is:

$$\begin{bmatrix} X_e - C \\ \theta_e \end{bmatrix}_{5 \times 1} = 0 \quad (9)$$

In the above set of equations  $C$  is a constant,  $X_e$  includes three elements of the edge position in contact with the ground and  $\theta_e$  consists of two elements of orientation around the  $x$  and  $z$  directions. The forces and moments exerted on this edge are:

$$f_e = \begin{bmatrix} F_e \\ M_e \end{bmatrix}_{5 \times 1} \quad (10)$$

As is mentioned for the constraints acting on the rotating foot, because the foot can rotate around the edge in contact with the ground surface, there is no moment acting around the  $y$  direction. Hence  $M_e$  just includes moments about the  $x$  and  $z$  directions. Similarly, because there is no moment acting around the  $y$  direction, the Jacobian matrix excluding this element can be written as:

$$J_e = \begin{bmatrix} J_v \\ J_\omega \end{bmatrix}_{5 \times 24} \quad (11)$$

By substituting the last two equations into Equation 2 and Equation 3, the dynamics model for the double support phase can be obtained:

$$\begin{aligned} M_{24 \times 24}(q) \ddot{q}_{24 \times 1} + C_{24 \times 1}(q, \dot{q}) + G_{24 \times 1}(q) \\ = B_{24 \times 18} \tau_{18 \times 1} + J_s^T J_{s6 \times 6} f_{s6 \times 1} + J_e^T J_{e5 \times 5} f_{e5 \times 1} \end{aligned} \quad (12)$$

By defining the Jacobian matrix for both feet in one matrix:

$$J = \begin{bmatrix} J_s \\ J_e \end{bmatrix}_{11 \times 24} \quad (13)$$

Equation 12 can be written as:

$$\begin{aligned} M_{24 \times 24}(q) \ddot{q}_{24 \times 1} + C_{24 \times 1}(q, \dot{q}) + G_{24 \times 1}(q) \\ = B_{24 \times 18} \tau_{18 \times 1} + J_{24 \times 11}^T f_{11 \times 1} \end{aligned} \quad (14)$$

In this case the unknown variables are more than equations. Because there is actuation redundancy, one possible solution is using Moore-Penrose inverse (Pseudo inverse) to solve the set of equations for actuating torques and contact forces, and moments with minimum 2-norm:

$$\begin{bmatrix} \tau_a \\ f_s \end{bmatrix}_{29 \times 1} = \begin{bmatrix} B & J_s^T \end{bmatrix}_{29 \times 24}^\# \left( M_{24 \times 24}(q) \ddot{q}_{24 \times 1} + C_{24 \times 1}(q, \dot{q}) + G_{24 \times 1}(q) \right) \quad (15)$$

In this equation  $[\ ]^\#$  is the pseudo inverse of the matrix.

### 2.3. Model verification

Because the robot has so many degrees of freedom, the procedure of developing equations of motion is error-prone. Thus, it seems vital to verify the dynamics model. In order to encapsulate the set of equations of motion, we use two analytical methods, i.e., Lagrange and Kane [26]. In order to verify the dynamics model, sinusoidal trajectories for all the joints are considered. It seems necessary to be noted that this set of trajectories does not result in a feasible motion for the robot and is just considered to apply a wide range of negative and positive values in the joint space.

In Figure 2 the obtained results from the two methods and the error between the two methods for the hip joint are shown. As can be

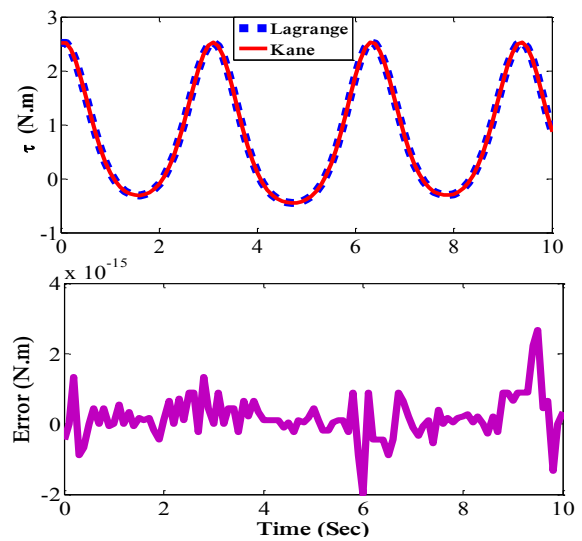


Fig. 2. Hip joint actuating torque and the error between the Lagrange and Kane methods

observed from these figures, both methods yield the same results and the error between them (of the order of  $10^{-15}$ ) is due to the computation round off. It should be noted that in the rest of this research, Kane's method is used anywhere a dynamics model is needed because of its lower calculation burden.

### 3. Slippage Effects

In order to obtain a better insight into the problem of slip on the bipedal robot feet during motion, we categorize this problem into two parts. The first considers suitable constraints on the robot's feet, in gait planning, to reduce the probability of the occurrence of slippage. The second part exploits sensory data and uses reflexive actions to prevent the robot from tipping over during real implementation [21]. In fact, in the presence of inevitable uncertainties, some unexpected disturbances may cause the robot to slip. The main aim of this section is to consider the slippage effects that should be taken into account during the gait planning procedure.

In the offline gait generation procedure, the gaits can be designed without considering slippage effects. Then, in the post processing procedure, the obtained gait should be checked to satisfy the slip constraints. However, this approach cannot be used in real time planning because of its huge computation burden. Hence, taking into account slip constraints during real time gait generation is a controversial challenge.

The forces that act on the stance foot of a biped from the ground are distributed over the stance foot (feet). These forces can be replaced by an overall force that is located on the COP of the foot (feet). This force vector is composed of horizontal and vertical components. The horizontal force should provide the necessary amount needed for slippage avoidance. The greater the friction coefficient between the foot and the ground, the more force there is that can be applied by the ground. As a result, the foot mechanism should be such that it provides enough friction forces [27].

The friction cone can provide better insight for slip analysis. This cone specifies the permissible bound for the forces that can be applied by the ground surface. The angle ( $\alpha$ ) of the friction cone that is shown in Figure 3a is a

function of the friction coefficient. This relation may be represented as:

$$\mu_s = \tan \alpha \quad (16)$$

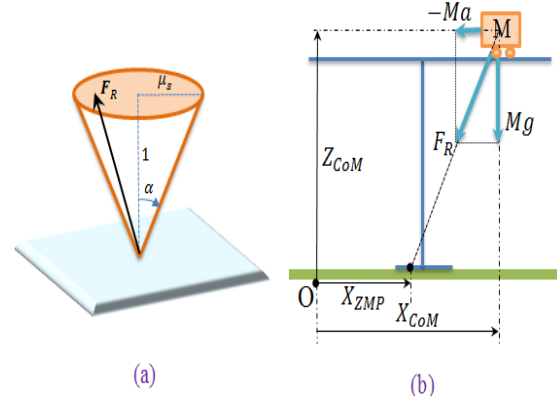


Fig. 3. a) Friction cone: a bound for interacting forces, b) Cart-table model

As long as the overall force that is exerted from the stance foot to the ground is within the friction cone, the foot would not slip. Thus, the lower the horizontal force applied by the stance foot, the lower the possibility of the occurrence of a slip is. The horizontal force that is transmitted to the ground surface is equal to the rate of change of the linear momentum of the whole body. A simple cart-table model [23] can be exploited to relate this problem. As is shown in Fig. 3b, in this simple model the COG of the robot can move on the table within a permissible bound. As can be observed, a higher acceleration of the cart can produce a higher amount of horizontal force from the base to the ground. Thus, in the procedure of gait planning the rate of the change of the linear momentum of the robot should be alleviated to reduce the horizontal forces that are needed to exert from the stance foot to the ground. This is the key point of the proposed gait planning approach that will be more discussed in section 4.1.3. Furthermore, because the support polygon boundary in SSP is lower than in DSP, the slip possibility in this phase is more than the DSP. As a result, in the rest of this paper our main focus is on the SSP.

### 4. Gait Planning

The task space of the lower body of the bipedal robot is composed of two segments, the pelvis and the feet. After designing trajectories for the feet to perform the desired walking pattern, the

feasibility constraints should be satisfied. By choosing the pelvis trajectory based on a COM trajectory, the feasibility of motion would be fulfilled and the walking pattern in the task space would be completed. Finally, using inverse kinematics [16], the task space trajectories can be projected into the joints space.

#### 4.1 Swing foot reference trajectory

There are lots of topologies that can be exploited for the motion of bipedal robots. These topologies depend on the foot mechanism of the robot and either the foot is equipped with the toe joint or not. For the under-study robot, there is no toe joint in the structure of the foot. As a result, the heel-toe-off topology without a toe joint [7] is adopted according to Figure 4.

#### 4.2 Reference ZMP and COM trajectories

The dynamics model that was obtained in section 2 is so complicated that it cannot be used in real-time procedures. In order to use a simple model to generate a feasible walking pattern for the biped robot, LIPM [9] can be adopted. Using this model, a linear equation that makes relations between the COM and the ZMP of the biped robot is available, and this equation can be solved to obtain a COM trajectory for a predefined ZMP trajectory.

The equations of the motion for a single inverted pendulum attached to the flat ground at a non-slipping contact point with fixed height are [9]:

$$\begin{cases} p_x = c_x - \frac{z_c}{g} \ddot{c}_x \\ p_y = c_y - \frac{z_c}{g} \ddot{c}_y \end{cases} \quad (17)$$

In this set of equations,  $p_x$  and  $p_y$  are the ZMP coordinates,  $c_x$  and  $c_y$  are the COM coordinates,  $z_c$  is the height of the pendulum and  $g$  represents the gravity constant. As was mentioned, in order to generate a feasible motion for the biped robot, the ZMP should lie inside the support polygon. Depending on what the trajectory for ZMP is considered as being, the COM trajectory and hence the overall motion becomes different. Three approaches are considered in the following.

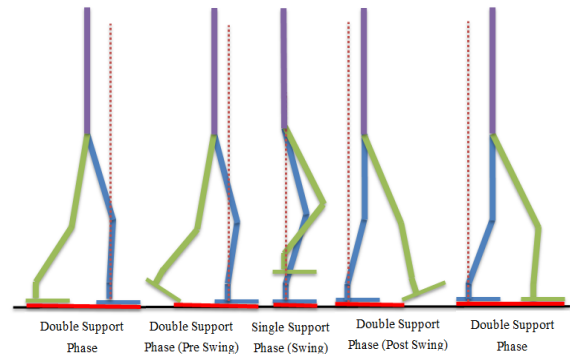


Fig. 4. Heel-toe-off topology without a toe or heel joint

##### 4.2.1. Approach (I): fixed ZMP

One of the most common approaches is when the ZMP is considered in the middle of the foot touching the ground. This approach is used by many authors. [25,28] This approach is suitable for implementation with a low level control in a joint space or a task space, with slight modifications to the feedback control. Although this approach provides a high stability margin during motion, there are many shortcomings which suggest that this method is not suitable. By using this method, not only do undesired fluctuations appear, but also high speed motion cannot be achieved.

##### 4.2.2. Approach (II): moving ZMP

Inspections of human walking [6] reveal that the ZMP is not fixed and moves from heel to toe during human walking. Because the best index for the naturalness of humanoid robot motion is its resemblance to human motion, it can be suggested that ZMP moves inside the support polygon. This method is used by many authors using various trajectories for ZMP [10,15,29,30].

In the moving ZMP approach, selecting the reference trajectory for the ZMP is a challenging problem. In the direction of the motion, an odd function, i.e., a first or third (or higher) order polynomial can be exploited as the desired trajectory for the ZMP in SSP. In this paper, the ZMP trajectory selected as a first order polynomial which moves from heel to toe. After designing a reference trajectory for the ZMP, Equation 17 is exploited to compute the COM trajectory. Using a Fourier transform and a Lanczos sigma as described in [10], these equations can be solved for the COM trajectory, analytically.

#### 4.2.3. Approach (III): low friction demanding moving-ZMP, LFDM

As was mentioned, the constraint on the ZMP trajectory is that this point should lie inside the support polygon during walking. However, this constraint only guarantees that the stance foot would not rotate around its edges. The other constraint is that the stance foot should not slip during walking. Thus, in order to fulfil both constraints, the two previously mentioned approaches cannot be exploited. The reason is that these approaches' design the reference ZMP trajectory at first and then calculate the COM reference trajectory, using the LIPM equations. The obtained COM trajectory only satisfies the ZMP constraints and cannot deal with slip constraints. As a result, the proposed approach is based on designing the COM trajectory which not only demands a low friction coefficient for walking, but also keeps the ZMP inside the support polygon.

Based on the discussions in section 2, in order to obtain a walking pattern with a low demanded friction coefficient, accelerations on the COM trajectory should be alleviated. The best option is a walking pattern with a constant speed for the COM. In such conditions, referring to Equation 18, the ZMP and COM trajectories in the frontal direction will coincide:

$$\dot{c}_x = \dot{p}_x = V \Rightarrow c_x = p_x = Vt + v_0 \quad (18)$$

where  $V$  is the constant speed and  $v_0$  is its initial velocity. Furthermore,  $c_x$  and  $p_x$  represent the COM and the ZMP trajectory in the frontal direction, respectively. Using this trajectory for the COM, its acceleration during motion would be zero and this motion demands a minimum friction coefficient among all the feasible motions that are obtained from the LIPM. In order to satisfy the ZMP constraints, the projection of the COM trajectory should lie inside the support polygon. However, in order to have a constant speed for the COM, the slope ( $V$ ) of the COM trajectory should be the same during both SSP and DSP. This factor is limited by the foot length and the DSP time span. In fact, if the foot length of the robot is large in comparison with the step length and the DSP time span is considered large enough during the walking pattern generation, it would

be possible to implement such a motion. However, if the projection of the COM trajectory on the ground in this method is outside of the borders of the support polygon, some modifications should be made. Under such circumstances, the COM trajectory is designed piecewise linear, whereby during the DSP, the projection of the COM moves to coincide with the heel (or the vicinity of the heel) of the stance foot of the SSP. Then during the SSP, the projection of the COM moves to the toe on a linear trajectory and so on. Both situations can be embedded in one equation:

$$\begin{cases} \dot{c}_{x,ss} = \dot{c}_{x,ds} = V, & \text{if } V \leq \frac{l_f}{T_{ss}} \\ \dot{c}_{x,ss} = \frac{l_f}{T_{ss}} \\ \dot{c}_{x,ds} = \frac{(T_{ss} + T_{ds})V - T_{ss}\dot{c}_{x,ss}}{T_{ds}}, & \text{else} \end{cases} \quad (19)$$

In this set of equations,  $\dot{c}_{x,ss}$  and  $\dot{c}_{x,ds}$  are the velocity of COM during SSP and DSP, respectively. Furthermore,  $l_f$ ,  $T_{ss}$ ,  $T_{ds}$  represent the foot length and SSP and DSP time span. The transition trajectory between the SSP and DSP of COM can be fitted by a fifth order polynomial to provide continuity in velocity and acceleration during motion. In this approach, after designing a COM trajectory, the ZMP will be checked with respect to whether it is inside the support polygon. Otherwise, the slope of the COM trajectory in the SSP is reduced to generate a feasible walking pattern. This procedure is shown in Figure 5. In the under-study robot, because the legs are small, designing large gaits is not possible. Furthermore, because the support polygon is relatively large, it is possible to design a linear trajectory for the COM with the same slope for both SSP and DSP.

In this approach, because the inverted pendulum equations are exploited to solve the ZMP, while the COM trajectory is given from Equations 19, the height of the COM does not need to be fixed. In fact, because in this case, the algebraic equations should be solved rather than differential equations to compute the ZMP, the original nonlinear equations of the inverted pendulum are considered:

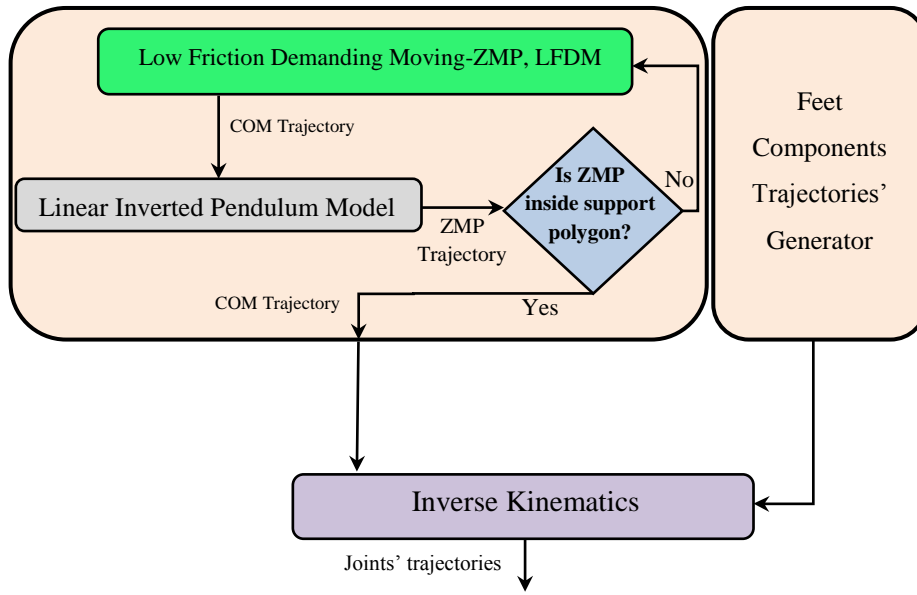


Fig. 5. Procedure of gait planning in proposed approach as Low Friction Demanding Moving-ZMP, LFD

$$\begin{cases} p_x = c_x - \frac{z_c}{g + z_c} \ddot{c}_x \\ p_y = c_y - \frac{z_c}{g + z_c} \ddot{c}_y \end{cases} \quad (20)$$

5. Obtained Results

The parameters of the under-study robot are taken from the kid-size robot, called the bioloid. The geometric parameters of this robot, including the lengths of the links, are given in Table 1. In Table 2 the gait parameters for walking with a speed of 22 cm/s are specified.

Table 1. The geometric parameters of the under-study robot

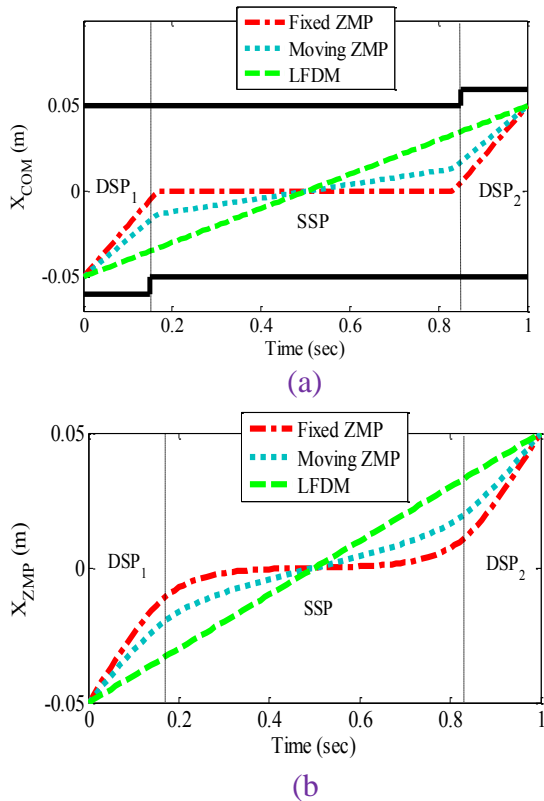
Parameter	Description	Quantity(cm)
$L_a$	Distance between foot and ankle joints' intersection	3.20
$L_{sh}$	Length of shank link	7.63
$L_{th}$	Length of thigh link	7.63
$L_h$	Distance between pelvis and hip joints' intersection	2.9
$L_p$	Length of pelvis link	4.85
$L_f$	Length of the foot	10
$w_f$	Width of the foot	6

Table 2. Gait parameters for 22cm/s speed of walking

Parameter	Description	Quantity
$T_{SS}$	Time span of SSP	0.7 (sec)
$T_{Ds}$	Time span of DSP	0.3 (sec)
$T_c$	Time span of a step	1 (sec)
$L_g$	Step length	22 (cm)
$w_g$	Step width	7.7 (cm)
$H_g$	Max. height of swing foot	3 (cm)
$\gamma_p$	Yaw angle of pelvis	30 (deg)

In this section we aim to compare the three approaches that are considered in section 4 in terms of slippage considerations. Gaits with various speeds for each approach are considered. In Figure 6 the ZMP and COM trajectories for walking with 22 cm/s speed are shown. In these figures “fixed ZMP”, “moving ZMP” and “low friction demanding moving ZMP” (LFD) are compared. As can be seen from Figure 6 (a), the ZMP moves from the heel to the toe during the SSP of the moving ZMP approaches, while in the fixed ZMP approach, the ZMP is fixed in the midpoint of the stance foot. Using the LIPM, the related COM trajectories of these approaches are

shown in Figure 6 (b). It can be observed from this figure that the closer the ZMP is to the midpoint of the stance foot, the more fluctuations there are that can be observed in the COM trajectory. These fluctuations not only disturb the resemblance of the walking pattern to human motion, but also could result in fluctuations of the forces between the stance foot and the ground surface. As is specified in these figures, the DSP is divided into two sub-phases, i.e., DSP<sub>1</sub> and DSP<sub>2</sub> in which the trailing foot rotates around its toe and the leading foot rotates around its heel, respectively (Fig. 4). It is noteworthy that in the lateral direction, the ZMP and COG trajectories for the three approaches are considered the same.



**Fig. 6. The ZMP and the COM trajectories for three approaches**

In Figure 7 the schematic representation of the walking of the three approaches during one step is presented. An inspection of these figures reveals that in the fixed ZMP approach, in which there are lots of fluctuations in the COM trajectory in the frontal direction, the upper body motion is interrupted and some

undesired fluctuations can be observed. Furthermore, in this approach, the harmony between leg and upper body motion is violated.

In the second approach, the ZMP in the direction of motion moves slightly from the back to the forth of the midpoint of the stance foot. In this approach, undesired fluctuations in the upper body motion are alleviated and the motion comes closer to the human walking. In the proposed LFDM approach in which the ZMP moves from the vicinity of the heel to toe during the SSP, the harmony between swing leg and upper body motion is satisfactory. A comparison between these three approaches suggests that the greater the trajectory of the ZMP is, the closer the ZMP trajectory is to the straight line from heel to toe, the better the motion resembles human walking.

The horizontal resultant force exerted from the stance foot to the ground surface is composed of  $x$  and  $y$  direction components. Because the trajectories for the COM in the lateral direction are considered the same for all three approaches, in order to compare the effects of the upper body motion in the saggital direction on motion feasibility, the  $x$  component of the interaction force is calculated, using the dynamics model obtained in section 2 and shown in Figure 8a for the three approaches. Comparing the graphs reveals that in the proposed LFDM approach, there are fewer fluctuations in the upper body motion compared with the other two approaches and the forces that are exerted from the foot to the ground surface are less. As a result, this approach is preferable in comparison with the others from the point of view of the occurrence of a slip. Furthermore, this force, during the first and last moments of the SSP, is more critical than the other moments of the gait.

The other component that should be taken into consideration is the vertical moment of interaction. This component would be more crucial when the walking speed is relatively high. In Figure 8b the vertical moment applied from the stance foot to the ground surface in the SSP during one step is drawn. Comparing these three approaches suggests that the fluctuations and accelerations of the upper body increase this moment. As can be observed, the vertical moment during the first and last moments of the SSP is more critical

than the other moments of a gait. Furthermore, in the proposed LFDM approach, this moment is lower than in the other approaches and a

lower friction coefficient is needed to implement this motion.

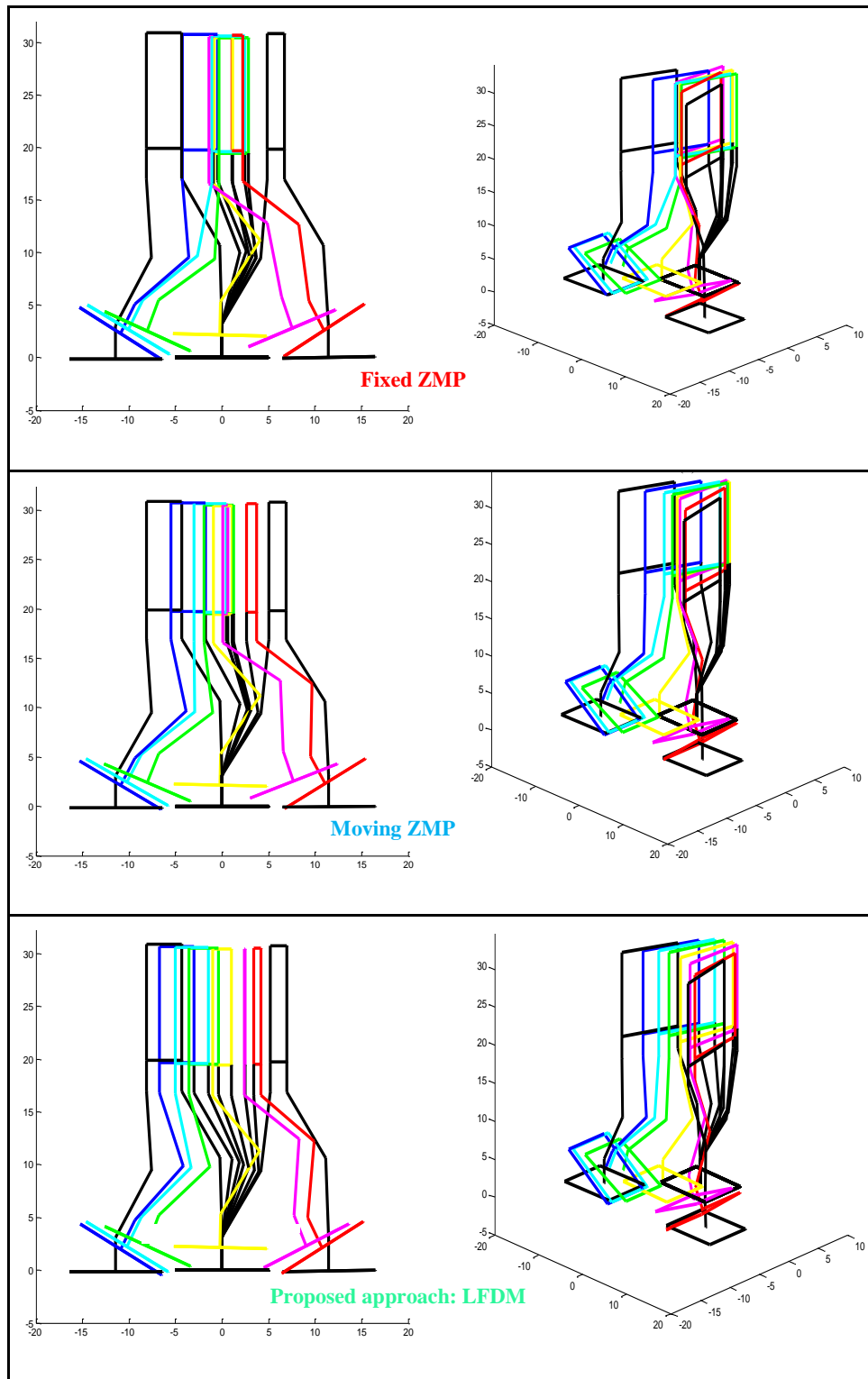


**Fig. 7.** An animated view of walking for three approaches during one step

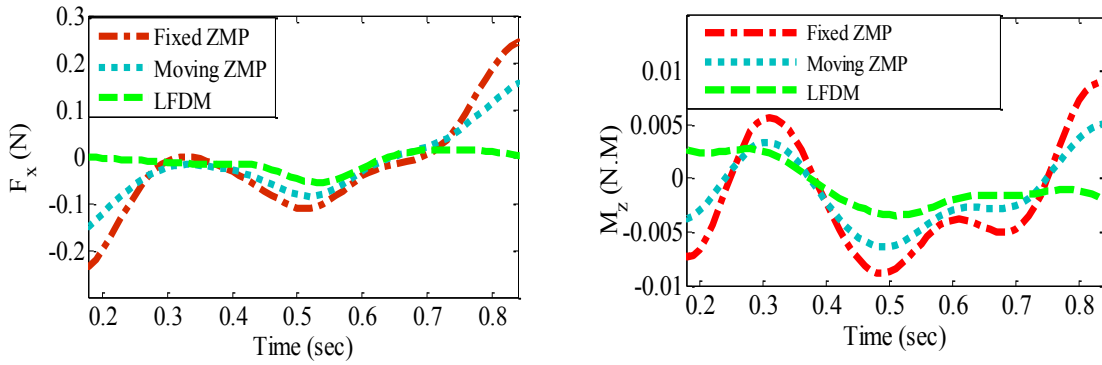


Fig. 8. Interaction frontal force and vertical moment for three approaches

In order to observe the role of the walking speed on the demanding friction coefficient needed to implement specified walking patterns, in Figure 9 the peak value of the minimum demanding friction coefficient during one step at various walking speeds is shown for the three approaches. As can be seen, increasing the walking speed demands a higher friction coefficient. Furthermore, gaits that are generated using the proposed LFDM approach require a lower friction coefficient.

The values that are obtained for the demanding friction coefficient to implement a feasible motion in Figure 9 are comparable to

the simulation and implementation results in [23]. In that study, the authors professed that they succeeded in implementing a walking pattern with a 1.24 Km/h speed on a slippery surface with a friction coefficient of 0.14. Furthermore, they related that according to their simulations, their robot can walk on a surface with a friction coefficient of 0.1. The approach that they exploited to generate a feasible walking pattern is a fixed ZMP. Thus, this paper proposes that by using a LFDM rather than a fixed ZMP in the direction of motion, the demanding friction coefficient would be alleviated.

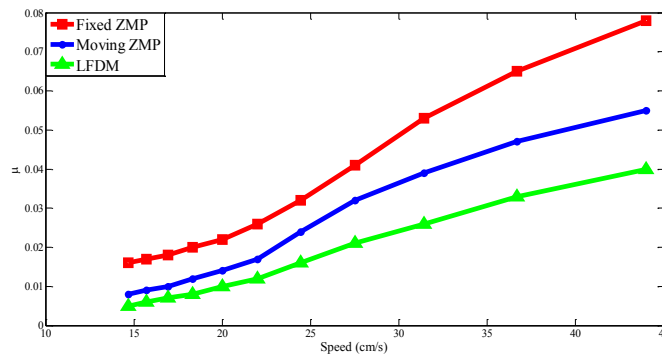


Fig. 9. A peak value of a minimum demanding friction coefficient during one step at various walking speeds

### 6. Conclusions

In this study, the effects of upper body motion on horizontal interaction forces and the vertical moment of a biped robot were studied. The proposed approach (LFDM) was compared with the two well-known approaches (fixed ZMP and moving ZMP) in terms of the demanding friction coefficient. Comparing these approaches with various walking speeds reveals that the greater the acceleration on the upper body motion, the greater the friction coefficient that is needed to implement feasible

motion. However, the proposed LFDM approach demands a lower friction coefficient than the others. Furthermore, it was shown that the proposed LFDM approach leads to a smoother upper body motion while it requires an almost constant friction coefficient during the SSP. Furthermore, the other two approaches are more vulnerable to causing slippage at the beginning and end of the SSP, due to the fact that they demand higher values of horizontal forces and vertical moment.

## References

- [1]. M. Rostami and G. Bessonnet, Sagittal gait of a biped robot during the single support phase. Part 2: optimal motion. *Robotica*. 2001;19:241–253.
- [2]. G. Capi, Y. Nasu, L. Barolli, K. Mitobe, and K. Takeda, Application of genetic algorithms for biped robot gait synthesis optimization during walking and going up-stairs. *Adv. Rob.* 2001;15:675–694.
- [3]. G. Bessonnet, P. Seguin, and P. Sardain, A parametric optimization approach to walking pattern synthesis. *Int. J. Rob. Res.* 2005;24:523–536.
- [4]. M. Vukobratović and B. Borovac, Zero-moment point-thirty five years of its life. *Int. J. Hum. Rob.* 2004;1:157-173.
- [5]. Goswami, Postural stability of biped robots and the foot-rotation indicator (FRI) point. *Int. J. Rob. Res.* 1999;18:523–533.
- [6]. M. B. Popovic, A. Goswami, and H. Herr, Ground reference points in legged locomotion: Definitions, biological trajectories and control implications. *Int. J. Rob. Res.* 2005;24:1013–1032.
- [7]. Q. Huang, K. Yokoi, S. Kajita, K. Kaneko, H. Arai, N. Koyachi, and K. Tanie, Planning walking patterns for a biped robot. *IEEE Trans. Rob.* 2001;17: 280-289.
- [8]. V. H. Dau, C. M. Chew, and A. N. Poo, Achieving energy-efficient bipedal walking trajectory through GA-based optimization of key parameters. *Int. J. Hum. Rob.* 2009;6: 609-629.
- [9]. S. Kajita, F. Kanehiro, K. Kaneko, K. Fujiwara, K. Yokoi, and H. Hirukawa, Biped walking pattern generation by a simple three-dimensional inverted pendulum model. *Adv. Rob.* 2003;17:131-147.
- [10]. K. Erbatur and O. Kurt, Natural ZMP trajectories for biped robot reference generation. *IEEE Trans. Ind. Elec.* 2009;56:835-845.
- [11]. S. A. A. Moosavian, M. Alghooneh, and A. Takhmar, Cartesian approach for gait planning and control of biped robots on irregular surfaces. *Int. J. Hum. Rob.* 2009;6:675-697.
- [12]. H. P. Huang, J. L. Yan, and T.H. Cheng, State-incremental optimal control of 3D COG pattern generation for humanoid robots. *Adv. Rob.* 2013;27:175-188.
- [13]. W. Suleiman, F. Kanehiro, K. Miura, and E. Yoshida, Enhancing zero moment point-based control model: system identification approach. *Adv. Rob.* 2011;25:427-446.
- [14]. J. H. Park and K. D. Kim, Biped robot walking using gravity-compensated inverted pendulum mode and computed torque control, In: Proceedings of the 1998 IEEE International Conference on Robotics and Automation; 1988. p. 3528-3533.
- [15]. T. Sato, S. Sakaino, and K. Ohnishi, Real-time walking trajectory generation method with three-mass models at constant body height for three-dimensional biped robots. *IEEE Trans. Ind. Elec.* 2011;58:376-383.
- [16]. M. Khadiv and A. A. Moosavian, A New Approach in Gait Planning for Humanoid Robots. In: Proceedings of the First RSI/ISM International Conference on Robotics and Mechatronics (ICRoM); 2013. p.171-177.
- [17]. S. A. A. Moosavian, M. Alghooneh, and A. Takhmar, Modified transpose Jacobian control of a biped robot, In: Proceedings of the 7th IEEE-RAS International Conference on Humanoid Robots; 2007. p. 282-287.
- [18]. H. O. Lim, S. A. Setiawan, and A. Takaniishi, Position-based impedance control of a biped humanoid robot. *Adv. Rob.* 2004;18:415-435.
- [19]. S. A. A. Moosavian, M. Alghooneh, and A. Takhmar, Introducing a Cartesian approach for gait planning and control of biped robots and implementing on various slopes. In: Proceedings of the 7th IEEE-RAS International Conference on Humanoid Robots; 2007. p. 545-550.
- [20]. K. Miura, F. Kanehiro, K. Kaneko, S. Kajita, and K. Yokoi, Slip-Turn for Biped Robots, *IEEE Trans. Rob.* 2013;29:875-887.
- [21]. G. N. Boone and J. K. Hodgins, Slipping and tripping reflexes for bipedal robots, *Auton. rob.* 1997;4:259-271.
- [22]. O. Kwon and J. H. Park, Reflex control of bipedal locomotion on a slippery surface. *Adv. Rob.* 2002;16:721-734.
- [23]. S. Kajita, K. Kaneko, K. Harada, F. Kanehiro, K. Fujiwara, and H. Hirukawa, Biped walking on a low friction floor, In: Proceedings of the 2004 IEEE/RSJ International Conference on Intelligent Robots and Systems, 2004. p. 3546-3552.

- [24]. K. Kaneko, F. Kanehiro, S. Kajita, M. Morisawa, K. Fujiwara, K. Harada, and H. Hirukawa, Slip observer for walking on a low friction floor, In: Proceedings of the 2005IEEE/RSJ International Conference on Intelligent Robots and Systems, 2005. p. 634-640.
- [25]. X. Zhou, Y. Guan, L. Jiang, H. Zhu, C. Cai, W. Wu, and H. Zhang, Stability of biped robotic walking with frictional constraints. *Robotica*. 2013;1:1-16.
- [26]. H. Baruh, *Analytical dynamics*: WCB/McGraw-Hill Boston, 1999.
- [27]. T. Buschmann, S. Lohmeier, and H. Ulbrich, Humanoid robot Lola: Design and walking control. *Jour. Physio*. 2009;103:141-148.
- [28]. H. Hirukawa, S. Kajita, F. Kanehiro, K. Kaneko, and T. Isozumi, The human-size humanoid robot that can walk, lie down and get up. *Int. J. Rob. Res.* 2005;24:755-769.
- [29]. S. A. A. Moosavian, A. Takhmar, and M. Alghooneh, Regulated sliding mode control of a biped robot, In: Proceedings of the 2007 ICMA International Conference on Mechatronics and Automation, 2007. p. 1547-1552.
- [30]. W. Park, J. Y. Kim, and J. H. Oh, Online walking pattern generation and its application to a biped humanoid robot—KHR-3 (HUBO), *Adv. Rob.* 2008;22:159-190.